Journal of Biosciences and Medicines, 2026, 14(4), 306-319
https://www.scirp.org/journal/jbm
ISSN Online: 2327-509X
ISSN Print: 2327-5081

# The Role of Ferroptosis and the Associated Gene CDKN1A in the Progression of Osteoarthritis

**Jinyou Nie[1], Fei Dou[1], Taoxian Wang[1], Rongxin Meng[1], Zeyu Hou[1], Dinggui Lu[1,2*]**

[1]Graduate School, Youjiang Medical University for Nationalities, Baise, China
[2]Department of Orthopedic Surgery, The Affiliated Hospital of Youjiang Medical University for Nationalities, Baise, China
Email: *ludinggui@163.com

**How to cite this paper:** Nie, J.Y., Dou, F., Wang, T.X., Meng, R.X., Hou, Z.Y. and Lu, D.G. (2026) The Role of Ferroptosis and the Associated Gene CDKN1A in the Progression of Osteoarthritis. *Journal of Biosciences and Medicines*, **14**, 306-319.
https://doi.org/10.4236/jbm.2026.144023

**Received:** March 21, 2026
**Accepted:** April 26, 2026
**Published:** April 29, 2026



## Abstract

**Objective:** To investigate the role and diagnostic value of ferroptosis-related genes, especially Cyclin-Dependent Kinase Inhibitor 1A (CDKN1A), in osteoarthritis (OA), and to assess the causal relationship between iron metabolism and the disease. **Methods:** OA-related differentially expressed genes (DEGs) from the GEO database were intersected with ferroptosis-related genes from FerrDb V3. Functional insights were obtained via GO/KEGG enrichment and PPI network analysis. Diagnostic value was evaluated using ROC curves. Mendelian randomization assessed causality using ferritin and TSAT as exposures and OA as the outcome. *In vitro*, an inflammatory model was established by stimulating chondrocytes with IL-1$\beta$ with or without a ferroptosis inhibitor, and CDKN1A and Col2 expression were detected. **Results:** Nine ferroptosis-related DEGs were identified. Enrichment analysis implicated these genes in long-chain fatty acid metabolism. ROC curve analysis showed high diagnostic efficacy for CDKN1A. Mendelian randomization revealed a significant positive causal association between increased transferrin saturation and OA risk. *In vitro* experiments demonstrated that inflammatory stimulation significantly reduced CDKN1A and Col2 expression in chondrocytes, an effect partially reversed by ferroptosis inhibitor intervention. **Conclusion:** The ferroptosis-related gene CDKN1A is downregulated in OA cartilage and may contribute to chondrocyte injury, potentially through ferroptosis-related pathways. Iron metabolism disorders are causally linked to OA.

## Keywords

Osteoarthritis, Ferroptosis, CDKN1A, Bioinformatics, Mendelian Randomization

## 1. Introduction

Osteoarthritis (OA) is a chronic joint disorder characterized primarily by articular cartilage degeneration, synovial inflammation, and abnormal subchondral bone remodeling. It is a leading cause of joint dysfunction and reduced quality of life in the middle-aged and elderly populations [1]. With the accelerating global population aging, the disease burden of OA is expected to increase continuously, with projections estimating over 1 billion cases worldwide by 2050 [2]. Although the pathogenesis of OA is not fully elucidated, research indicates that chondrocyte death plays a critical role in disease progression. Ferroptosis, a form of programmed cell death characterized by iron-dependent lipid peroxidation, has garnered significant attention in this context [3]. Multiple studies have shown evidence of iron metabolism disorders and accumulation of lipid peroxidation products in OA cartilage tissue, suggesting that ferroptosis may be involved in the pathological process of OA [4].

Ferroptosis is a novel form of cell death distinct from apoptosis and necrosis. Its core feature is the excessive, iron-dependent accumulation of lipid peroxides, ultimately leading to cell membrane rupture [5]. This process is regulated by various genes, including glutathione peroxidase 4 (GPX4) and solute carrier family 7 member 11 (SLC7A11), and is closely linked to amino acid metabolism, lipid metabolism, and iron homeostasis [6]. In the OA field, studies suggest that abnormal iron metabolism may be associated with the development and progression of joint diseases. Mendelian randomization (MR) studies can utilize genetic variants as instrumental variables to infer causal relationships between exposures and disease outcomes, providing genetic evidence to elucidate the potential causal link between iron status and OA [7].

CDKN1A, encoding the p21 protein, is a crucial member of the cyclin-dependent kinase inhibitor family and plays a key regulatory role in processes such as cell cycle arrest, senescence, and apoptosis [8]. Recent studies have revealed that CDKN1A also participates in the ferroptosis regulatory network. For instance, MDM2 can mediate the ubiquitination of CDKN1A, downregulating its expression in chondrocytes, leading to impaired chondrocyte viability and inducing ferroptosis and oxidative stress [9]. Notably, in other disease models, CDKN1A has been identified as a key gene regulating endoplasmic reticulum stress-induced ferroptosis, further highlighting its central role in ferroptosis pathways [10]. However, the specific mechanism of CDKN1A in chondrocyte ferroptosis during OA requires further elucidation. This study integrates bioinformatics analysis, MR methods, and *in vitro* cellular experiments to systematically evaluate the role of ferroptosis-related genes, particularly CDKN1A, in OA progression, providing a theoretical basis for revealing OA pathogenesis and identifying potential therapeutic targets.

## 2. Materials and Methods

### 2.1. Data Acquisition

The OA dataset for this study was obtained from the Gene Expression Omnibus

(GEO) database (https://www.ncbi.nlm.nih.gov/geo/). The GSE114007 dataset [11] provides RNA-seq data from human knee cartilage. Normal samples (n = 18, 5F/13M, mean age 38 years, range 18 - 61) were obtained post-mortem from donors without joint disease. OA samples (n = 20, 12F/8M, mean age 66 years, range 52 - 82) came from knee replacement surgery. All samples were taken from weight-bearing femoral condyles. BMI was similar between groups (normal: 32.4 ± 8.0, OA: 30.7 ± 8.1, p = 0.506). Because raw counts were used for differential expression, no adjustment for age or sex was applied. Ferroptosis-related genes were sourced from the third version of the Ferroptosis Database (FerrDb V3) (http://www.zhounan.org/ferrdb/) [12], which systematically compiles information on regulators, drivers, and markers associated with ferroptosis. This yielded 1019 regulator genes, 731 driver genes, and 59 marker genes. After removing cross-category duplicates (153 genes), 1656 unique genes remained. The data for Mendelian randomization analysis were obtained from the IEU OpenGWAS platform (https://gwas.mrcieu.ac.uk/).

### 2.2. Differential Expression Gene Analysis

Differential expression analysis between OA and normal control groups was performed on the count data using the DESeq2 package in R software. Raw count data were used as input for DESeq2. Normalized counts were transformed with the regularized-logarithm function, and these regularized-logarithm-transformed values were used only for heatmap visualization. Significantly differentially expressed genes (DEGs) were identified using an adjusted P-value < 0.05 and an absolute log2 fold change > 1 as screening criteria. Volcano plot and Heatmap of the top 50 DEGs were generated to visualize gene expression differences between OA and normal samples. Subsequently, Weighted Gene Co-expression Network Analysis (WGCNA) was performed using the "WGCNA" package in R, but the WGCNA results were exploratory and did not contribute to the selection of ferroptosis-related DEGs. Gene Ontology (GO) functional enrichment analysis and Kyoto Encyclopedia of Genes and Genomes (KEGG) pathway enrichment analysis were then conducted on the DEGs.

### 2.3. Identification and Analysis of Ferroptosis-Related DEGs

After obtaining the 1656 unique ferroptosis-related genes from the FerrDb V3, we intersected them with the DEGs. The overlapping genes were defined as ferroptosis-related DEGs, no further filtering or prioritization was performed using WGCNA or other methods. A Venn diagram visualized the overlap. GO and KEGG enrichment analyses were performed on these ferroptosis-related DEGs, and the results are tabulated. Protein-protein interaction (PPI) network analysis was conducted using STRING database (http://string-db.org/) with a confidence level > 0.4 and visualized with Cytoscape (version 3.8.1); hub genes were identified using CytoHubba plugin. The expression levels of candidate genes were compared between the OA and control groups. Receiver operating characteristic (ROC)

curve analysis was performed using the dataset to evaluate the diagnostic value of candidate genes, and a nomogram was constructed.

### 2.4. Mendelian Randomization Analysis

To evaluate potential causal relationships between iron exposure and OA, MR analysis was conducted. The outcome was OA from a European population (sample size = 393,873). Exposures were serum ferritin (n = 23,986) and transferrin saturation (TSAT, n = 23,986), both from European populations. Instrumental variables for each exposure were selected using $P < 5 \times 10^{-8}$, clumping with $r^2 < 0.001$. The F-statistic for each IV exceeded 10, indicating strong instruments. For ferritin, 4 SNPs were retained; for TSAT, 3 SNPs were retained. The "TwoSampleMR" package in R software was used to perform MR analysis on the GWAS data from the exposure and outcome groups. Instrumental variables for exposures were selected using a significance threshold of P < 5e−08. The inverse variance weighted (IVW) method was used as the primary analysis model, with MR-Egger regression and weighted median methods applied for sensitivity analysis. Heterogeneity among instrumental variables was assessed using Cochran's Q test, and horizontal pleiotropy was assessed using the MR-Egger intercept test to verify the robustness of the analysis results.

### 2.5. Cell Culture and Intervention

Human chondrocytes used in this experiment were obtained from Procell Life Science & Technology Co., Ltd. (Wuhan, China; Cat# CP-H107). Cells were cultured in DMEM/F12 medium containing 10% fetal bovine serum and 1% penicillin/streptomycin in a humidified incubator at 37˚C with 5% $CO_2$. To simulate the inflammatory microenvironment of OA *in vitro*, chondrocytes were stimulated with interleukin-1$\beta$ (IL-1$\beta$) at a concentration of 10 ng/ml to establish an OA inflammation model. A ferroptosis inhibitor (Ferrostatin-1, 5 μM) was used for intervention for 72 hours. Cells were divided into three groups: control group, IL-1$\beta$ group, and IL-1$\beta$ + ferroptosis inhibitor group.

### 2.6. Quantitative Real-Time PCR (RT-qPCR)

Total RNA was extracted from cells using TRIzol reagent, followed by reverse transcription to synthesize complementary DNA (cDNA). Real-time quantitative PCR was performed using SYBR Green reagent. GAPDH was used as the internal reference gene, and relative expression levels were calculated using the 2^(-ΔΔCt) method. CDKN1A primer sequences were: F GCAGACCAGCATGACAGAT, R GAGACTAAGGCAGAAGATGTAG AG.

### 2.7. Immunofluorescence Staining

Chondrocyte type II collagen (Col2) expression was assessed. Chondrocytes grown on coverslips were gently washed 2 - 3 times with pre-warmed phosphate-buffered saline (PBS). Cells were fixed with 4% paraformaldehyde for 15 - 20

minutes at room temperature, then washed three times with PBS for 5 minutes each. Permeabilization was performed using 0.2% Triton X-100 for 10 - 15 minutes at room temperature, followed by three PBS washes for 5 minutes each. Cells were blocked with 10% goat serum for 60 minutes at room temperature. After removing the blocking solution, cells were incubated with diluted primary antibody (Col2, Proteintech Group, Inc., Cat No. 28459-1-AP, 1:200) overnight at 4˚C. Following primary antibody removal and three PBS with Tween-20 (PBST) washes, cells were incubated with a fluorophore-conjugated secondary antibody for 1 hour at room temperature in the dark. After three PBST washes in the dark, coverslips were mounted with an anti-fade mounting medium containing DAPI. After 5 minutes of incubation at room temperature in the dark, images were observed and captured using a confocal microscope.

### 2.8. Statistical Analysis

Statistical analysis was performed using R software (version 4.5.1) and GraphPad Prism (version 9.5.1). Comparisons between two groups were performed using a t-test, and comparisons among multiple groups were performed using one-way analysis of variance (ANOVA). The $P < 0.05$ was considered statistically significant.

## 3. Results

### 3.1. Identification of Differentially Expressed Genes

Analysis of the gene expression profiles from the GSE114007 dataset compared OA and normal cartilage tissue. A set of significantly differentially expressed genes was identified, with 1311 genes significantly upregulated and 936 genes downregulated in OA tissue. The volcano plot showed a distinct distribution of DEGs between the two sample groups (**Figure 1(A)**). The heatmap of the top 50 DEGs (**Figure 1(B)**) revealed clear differences in expression patterns between OA and normal samples, with samples clustering distinctly, suggesting these genes may be involved in the molecular regulatory processes of OA development. Further WGCNA was performed to construct a gene co-expression network. The scale independence plot (**Figure 1(C)** left) showed the relationship between the scale-free fit index ($R^2$) and the soft-threshold power, with a soft-threshold power of 7 selected. The mean connectivity plot (**Figure 1(C)** right) showed the relationship between mean connectivity and the soft-threshold power, used to assess network connectivity. The gene clustering dendrogram (**Figure 1(D)**) illustrated the clustering of genes based on expression similarity, corresponding to module colors. The dendrogram branches represented hierarchical clustering of genes, and the color bar below indicated modules identified by dynamic tree cutting. Genes were partitioned into different modules; genes within the same module showed highly correlated expression patterns. Module size and number reflected the co-expression structure. Genes enriched in the blue module, for example, might play important roles in OA development. The module-trait relationship heatmap (**Fig-**

ure 1(E)) displayed the correlation between each module's eigengene and external traits (OA status). Each cell represented the correlation coefficient and P-value for the module-trait relationship, with color intensity indicating correlation strength. The MEpurple module showed the highest positive correlation with OA, while the MEcyan module showed the highest negative correlation. But these WGCNA results were not used for downstream gene prioritization.

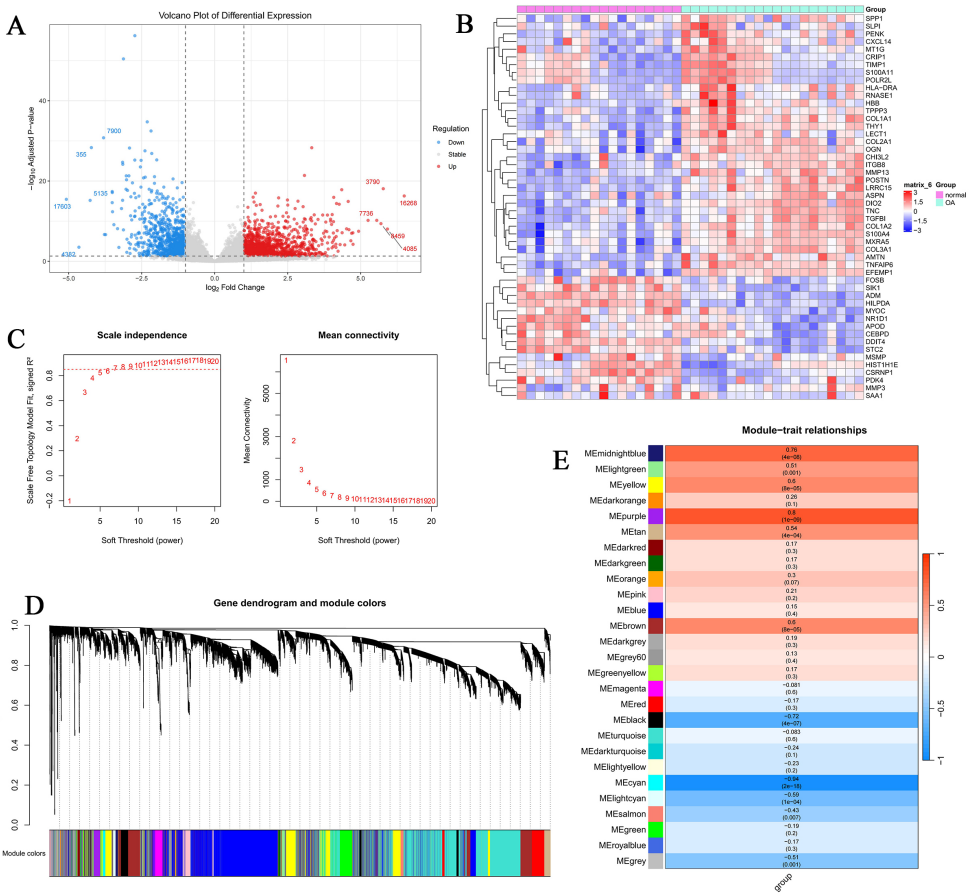


**Figure 1.** Identification of DEGs and WGCNA in OA. (A) Volcano plot of DEGs. (B) Heatmap of DEGs. (C) Soft-threshold power selection plots (scale independence and mean connectivity). (D) Gene clustering dendrogram. (E) Module-trait relationship heatmap.

## 3.2. Identification of Ferroptosis-Related DEGs

Ferroptosis-related genes were obtained from the FerrDb database and intersected with the identified DEGs, ultimately yielding 9 ferroptosis-related DEGs (**Figure 2(A)**): PTGS2, CHAC1, TF, CDKN1A, MT1G, SAT1, DPP4, ACSL4, and HSBP1. GO functional enrichment analysis (**Figure 2(B)**) indicated that these genes are primarily involved in the activation and metabolism of long-chain fatty acids, such as arachidonic acid, processes occurring on endoplasmic reticulum/mitochondrial membranes, and iron ion binding. The genes contributing to the top GO terms were: for "long-chain fatty acid metabolic process", ACSL4, PTGS2, CHAC1; for "iron ion binding", TF, PTGS2, CHAC1. KEGG pathway analysis

(Figure 2(C), Figure 2(D)) suggested that these genes are enriched in pathways related to iron homeostasis, HIF-1 signaling, and oxytocin signaling, which may be involved in the regulation of ferroptosis. Additionally, CDKN1A links to cellular senescence and cell cycle arrest, contributing to the pathological basis of OA. The GO and KEGG enrichment results for ferroptosis-related DEGs with P.adjust < 0.05 are shown in Table 1.

Table 1. GO and KEGG enrichment analysis of ferroptosis-related DEGs.

| Ontology | ID | GeneRatio | BgRatio | P value | P.adjust |
|---|---|---|---|---|---|
| BP | GO:0032310 | 2/9 | 17/18860 | 2.74e−05 | 0.0137 |
| BP | GO:0015732 | 2/9 | 28/18860 | 7.60e−05 | 0.019 |
| BP | GO:0042759 | 2/9 | 40/18860 | 0.0002 | 0.0236 |
| BP | GO:0032309 | 2/9 | 44/18860 | 0.0002 | 0.0236 |
| BP | GO:0140353 | 2/9 | 52/18860 | 0.0003 | 0.026 |
| MF | GO:0008199 | 1/9 | 10/18662 | 0.0048 | 0.0424 |
| MF | GO:0008239 | 1/9 | 10/18662 | 0.0048 | 0.0424 |
| MF | GO:0031957 | 1/9 | 10/18662 | 0.0048 | 0.0424 |
| MF | GO:0047676 | 1/9 | 11/18662 | 0.0053 | 0.0424 |
| MF | GO:0016840 | 1/9 | 12/18662 | 0.0058 | 0.0424 |
| KEGG | hsa04216 | 3/8 | 42/9370 | 4.61e−06 | 0.0003 |
| KEGG | hsa04978 | 2/8 | 61/9370 | 0.0011 | 0.0393 |

### 3.3. Protein-Protein Interaction Network and Hub Gene Identification

A PPI network of the ferroptosis-related DEGs was constructed using the STRING database and visualized with Cytoscape software. The PPI results (Figure 2(E)) showed relatively close interaction relationships among these genes. Further analysis using the CytoHubba algorithm (Figure 2(F)) indicated that ACSL4 had a high degree of connectivity in the network, along with CDKN1A, MT1G, SAT1, PTGS2, and CHAC1, suggesting these genes may play core roles in the ferroptosis regulatory network. Differential expression analysis of the candidate hub genes showed significantly reduced expression of CDKN1A in OA samples (Log2FC = −2.99). ROC curve analysis (Figure 2(G)) demonstrated that CDKN1A had strong diagnostic ability in distinguishing OA samples from normal samples (AUC = 0.975). A nomogram model was constructed based on the candidate genes (Figure 2(H)), showing good stability and predictive ability for assessing OA risk.

### 3.4. Mendelian Randomization Analysis

MR analysis was performed to further assess potential causal relationships between iron status and OA. The scatter plot for the MR analysis of ferritin exposure and OA outcome (Figure 3(A)) showed the effect distribution of individual Single Nucleotide Polymorphisms (SNPs) on ferritin levels and OA risk. The slope of the MR-Egger regression line was positive, and its intercept was close to zero (inter-

cept P > 0.05), suggesting no significant horizontal pleiotropy. However, the confidence interval for the IVW method's fit line was wide, and some SNPs appeared to have a larger influence on the outcome, potentially driving the causal effect estimate. The forest plot (**Figure 3(B)**) displayed the causal effect estimates of individual SNPs and different MR methods on ferritin and OA. The Wald ratio estimates for individual SNPs varied in direction, with some confidence intervals crossing the null line.

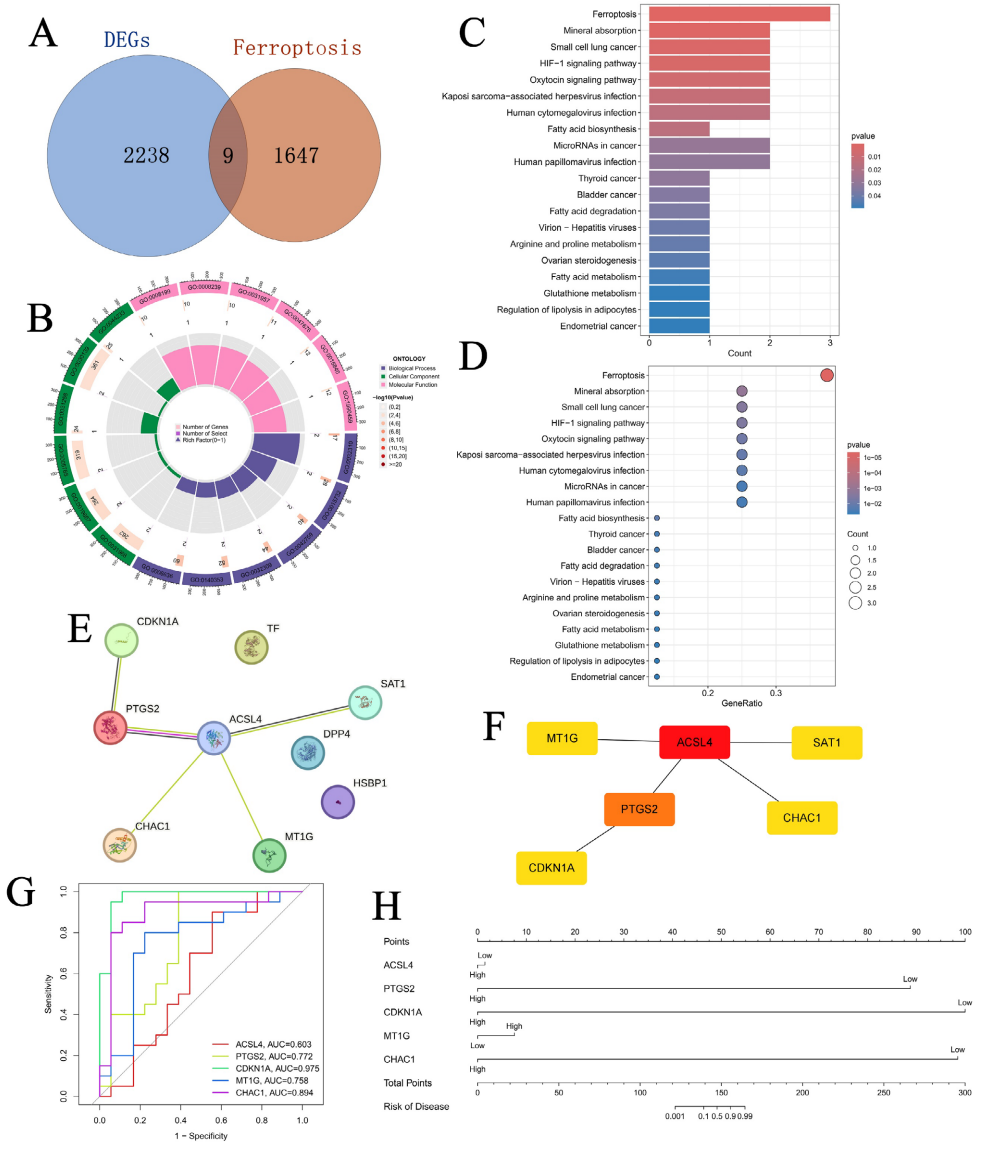


**Figure 2.** Identification and analysis of ferroptosis-related DEGs in OA. (A) Venn diagram of ferroptosis-related DEGs. (B) GO enrichment analysis plot. (C, D) KEGG pathway enrichment analysis plots. (E) PPI network diagram. (F) CytoHubba algorithm analysis results. (G) ROC curve for CDKN1A. (H) Nomogram for OA risk prediction.

The pooled effect estimate from the IVW method was OR = 1.36, 95% CI (0.97 - 1.91), P = 0.079. However, both the MR-Egger and weighted median methods

suggested a positive association between ferritin levels and OA risk (MR Egger: OR = 2.12, 95% CI (1.59 - 2.83), P = 0.036; Weighted median: OR = 1.26, 95% CI (1.01 - 1.58), P = 0.040). The MR-Egger intercept was not significant (P > 0.05), indicating no horizontal pleiotropy. Because MR-Egger is robust to pleiotropy, these results suggest that higher ferritin levels may increase OA risk. For TSAT (**Figure 3(C)**, **Figure 3(D)**), the weighted median and IVW methods reached statistical significance (weighted median: OR = 1.18, 95% CI 1.09 - 1.28, P = $3.5 \times 10^{-5}$; IVW: OR = 1.15, 95% CI 1.01 - 1.33, P = 0.042). MR-Egger showed a consistent direction but wider CI (OR = 1.27, 95% CI 0.998 - 1.60, P = 0.302). Overall, the results support a significant causal association between increased TSAT and increased OA risk.

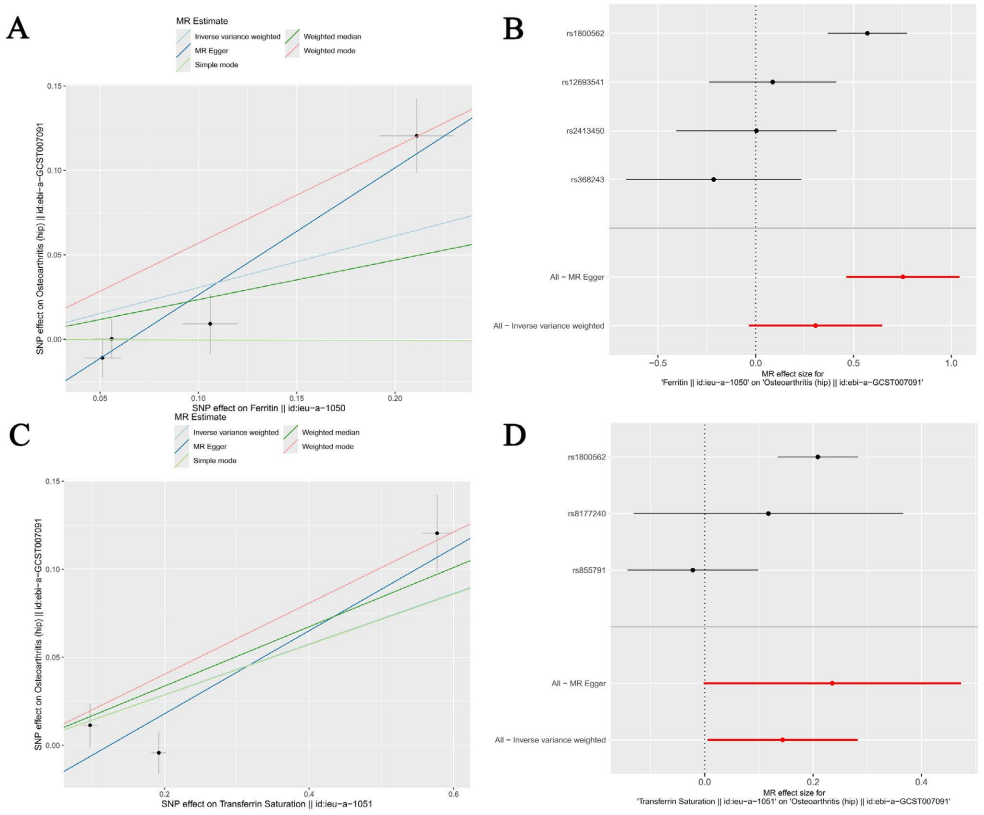


**Figure 3.** MR analysis of the causal association between iron status and OA risk. (A, B) Scatter plot and forest plot for MR analysis of ferritin exposure and OA outcome. (C, D) Scatter plot and forest plot for MR analysis of transferrin saturation exposure and OA outcome.

### 3.5. Effect of Inflammatory Stimulation on CDKN1A Expression in Chondrocytes

CDKN1A expression was detected in human chondrocytes after establishing an IL-1$\beta$-induced inflammation model. RT-qPCR results (**Figure 4(A)**) showed that CDKN1A expression levels were significantly lower in the inflammation stimulation group compared to the control group. Immunofluorescence staining results (**Figure 4(B)**, **Figure 4(C)**) showed changes in chondrocyte type II collagen ex-

pression, indicating that inflammatory stimulation could affect the chondrocyte phenotype.

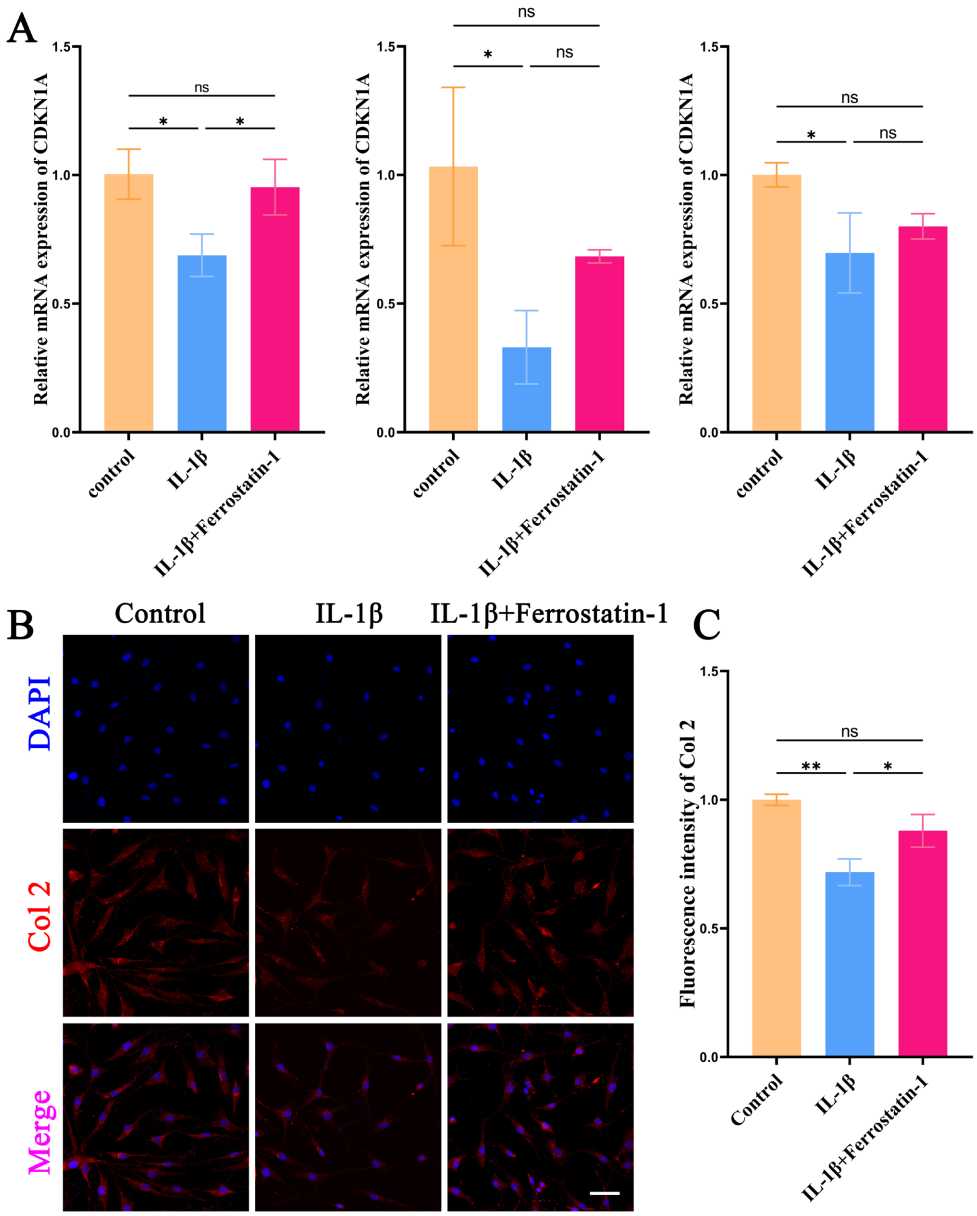


**Figure 4.** CDKN1A expression and Col2 immunofluorescence in chondrocytes under IL-1$\beta$ stimulation and ferroptosis inhibitor treatment. (A) Relative CDKN1A mRNA expression levels in each group (n = 3). (B, C) Immunofluorescence staining results for Col2 protein in each group and corresponding fluorescence intensity quantification. Scale bar = 50 μm. *P < 0.05, **P < 0.01.

### 3.6. Effect of Ferroptosis Inhibitor on Chondrocyte Injury

A ferroptosis inhibitor was added as an intervention alongside inflammatory stimulation. RT-qPCR results (**Figure 4(A)**) showed that CDKN1A expression levels increased. Immunofluorescence results (**Figure 4(B)**, **Figure 4(C)**) indicated that structural damage to chondrocytes was ameliorated to some extent, and

type II collagen expression levels partially recovered. These data suggest an association between the ferroptosis pathway and inflammation-induced chondrocyte injury, as the ferroptosis inhibitor Ferrostatin-1 partially rescued the phenotype. However, no direct markers of ferroptosis (e.g., lipid peroxidation, malondialdehyde, GPX4 activity) were measured; therefore, the results support a potential link rather than a definitive demonstration of ferroptosis in this model.

## 4. Discussion

This study systematically investigated the role of ferroptosis-related genes in OA, focusing on the potential function of CDKN1A, by integrating bioinformatics analysis, MR analysis, and cellular experimental validation. Based on DEG screening from the GSE114007 dataset, 1311 upregulated and 936 downregulated genes were identified. Intersection with FerrDb V3 ferroptosis-related genes yielded 9 ferroptosis-related DEGs, among which CDKN1A was significantly downregulated in OA cartilage tissue. This finding aligns with previous research suggesting that chondrocytes in an inflammatory microenvironment may exhibit abnormal cell cycle regulation, and the downregulation of p21, a key cyclin-dependent kinase inhibitor, might weaken cellular defense against oxidative stress [13]. PPI network analysis indicated that genes such as ACSL4, CDKN1A, PTGS2, and CHAC1 occupied central positions in the network, suggesting these genes may participate in OA pathogenesis through cooperative regulation of ferroptosis pathways [14]. GO and KEGG enrichment analyses further revealed that these genes are primarily involved in biological processes like long-chain fatty acid metabolism, iron ion binding, prostaglandin synthesis, and the HIF-1 signaling pathway, all closely associated with ferroptosis occurrence.

Notably, ROC curve analysis showed that CDKN1A possessed high diagnostic efficacy in distinguishing OA samples from normal samples, with an AUC of 0.975, suggesting its potential as a biomarker for OA. The construction of the nomogram model further validated the feasibility of a prediction model based on ferroptosis-related genes for assessing OA risk. Previous studies have shown that the p21 protein encoded by CDKN1A not only regulates the cell cycle but also participates in various biological processes such as cellular senescence, apoptosis, and DNA damage repair. Recent research has revealed its significant role in the ferroptosis regulatory network [15]. MDM2 can mediate the ubiquitination of CDKN1A, downregulating its expression in chondrocytes, leading to impaired chondrocyte viability and inducing ferroptosis and oxidative stress [9]. The cellular experiment results of this study are consistent with this; in the IL-1$\beta$-induced chondrocyte inflammation model, CDKN1A expression was significantly reduced, while the addition of a ferroptosis inhibitor partially restored its expression and improved chondrocyte type II collagen expression, suggesting that inhibiting ferroptosis might alleviate chondrocyte injury by upregulating CDKN1A expression.

The MR analysis provided genetic evidence supporting these findings. Results

showed a significant positive causal association between increased transferrin saturation and OA risk, with the weighted median method showing an OR of 1.18 and the IVW method also reaching statistical significance. The association between ferritin levels and OA was significant in MR-Egger and weighted median methods but not in the IVW method, possibly limited by a smaller number of instrumental variables or weak instrument bias. Overall, the MR results support a potential causal role for iron metabolism disorders, particularly elevated transferrin saturation, in OA pathogenesis [16]. This finding corroborates the ferroptosis pathway central to this study; iron, as a core element of ferroptosis, and alterations in its metabolic state may contribute to cartilage degeneration by influencing lipid peroxidation processes [17]. Previous studies have also indicated that iron overload can induce ferroptosis in chondrocytes, while iron chelators can mitigate inflammatory stimuli-induced chondrocyte injury [18].

This study has certain limitations. First, the bioinformatics analysis was based on a single GEO dataset with a relatively small sample size; validation in larger independent cohorts is needed. Second, the *in vitro* experiments did not measure direct ferroptosis markers such as lipid reactive oxygen species, malondialdehyde, or GPX4 activity; thus, while Ferrostatin-1 provided protective effects, we cannot conclusively state that ferroptosis occurred. Future studies should include these direct measurements. Third, the MR analysis for ferritin had a limited number of instrumental variables, which may affect precision. Fourth, this study focused on chondrocytes; the role of ferroptosis in other joint cell types requires further investigation. Fifth, the DEGs were derived from knee OA but the MR outcome was primarily hip OA; despite shared ferroptosis pathways, site-specific validation is needed.

In summary, through multi-omics integrated analysis combined with MR methods and cellular experimental validation, this study revealed the potential role of ferroptosis-related genes, particularly CDKN1A, in OA progression. The results indicate that CDKN1A is downregulated in OA cartilage tissue and may participate in chondrocyte injury by influencing ferroptosis pathways, while inhibiting ferroptosis can partially improve the cellular phenotype. The causal association between iron metabolism status and OA provides genetic evidence supporting the ferroptosis hypothesis. This study offers a new perspective for a deeper understanding of OA pathogenesis and lays a preliminary theoretical foundation for developing therapeutic strategies targeting ferroptosis regulation.

## 5. Conclusion

This study systematically evaluated the potential role of ferroptosis-related genes in osteoarthritis. Intersection analysis of DEGs screened from the GEO database and FerrDb ferroptosis genes identified CDKN1A as a potential key gene. Mendelian randomization analysis suggested a possible association between iron metabolism status and OA risk. Cellular experiments further demonstrated that inflammatory stimulation could induce decreased CDKN1A expression in chondro-

cytes, while inhibiting ferroptosis-like processes alleviated cell injury, although direct ferroptosis markers were not measured. The findings suggest that the ferroptosis-related gene CDKN1A may be involved in the pathological progression of OA and could serve as a potential molecular marker and therapeutic target.

## Acknowledgements

We thank the Gene Expression Omnibus database and the IEU OpenGWAS project for providing the datasets for analysis.

## Funding

This paper is supported by grants from the Guangxi Natural Science Foundation Project (No: 2023GXNSFAA026408 and 2025GXNSFHA069045).

## Conflicts of Interest

The authors declare that the research was conducted in the absence of any commercial or financial relationships that could be construed as a potential conflict of interest.

## References

[1] Tang, S., Zhang, C., Oo, W.M., Fu, K., Risberg, M.A., Bierma-Zeinstra, S.M., *et al*. (2025) Osteoarthritis. *Nature Reviews Disease Primers*, **11**, Article No. 10. https://doi.org/10.1038/s41572-025-00594-6

[2] Yuan, Y., Zhang, J., Zhang, P. and Nachin, B. (2026) Temporal Trends in Global Incidence of Musculoskeletal Disorders and Future Projections to 2050. *Asian Journal of Surgery*, In Press. https://doi.org/10.1016/j.asjsur.2026.02.061

[3] Xiao, J., Zhu, Y., Chen, J., Hong, Y. and Cao, Y. (2025) Ferroptosis at the Intersection of Osteoarthritis and Bone Metabolism: Mechanistic Links and Therapeutic Prospects. *Frontiers in Cell and Developmental Biology*, **13**, Article ID: 1722435. https://doi.org/10.3389/fcell.2025.1722435

[4] Xia, S., Li, L., Shi, Z., Sun, N. and He, Y. (2025) Ferroptosis in Osteoarthritis: Metabolic Reprogramming, Immunometabolic Crosstalk, and Targeted Intervention Strategies. *Frontiers in Immunology*, **16**, Article ID: 1604652. https://doi.org/10.3389/fimmu.2025.1604652

[5] Cao, S., Wei, Y., Yue, Y., Chen, Y., Qian, J., Wang, D., *et al*. (2024) Rosiglitazone Retards the Progression of Iron Overload-Induced Osteoarthritis by Impeding Chondrocyte Ferroptosis. *iScience*, **27**, Article 110526. https://doi.org/10.1016/j.isci.2024.110526

[6] Liu, Y., Zhang, Z., Fang, Y., Liu, C. and Zhang, H. (2024) Ferroptosis in Osteoarthritis: Current Understanding. *Journal of Inflammation Research*, **17**, 8471-8486. https://doi.org/10.2147/jir.s493001

[7] Wang, X., Qiu, L., Yang, Z., Wu, C., Xie, W., Zhang, J., *et al*. (2024) Association between Serum Iron Status and the Risk of Five Bone and Joint-Related Diseases: A Mendelian Randomization Analysis. *Frontiers in Endocrinology*, **15**, Article ID: 1364375. https://doi.org/10.3389/fendo.2024.1364375

[8] Manousakis, E., Miralles, C.M., Esquerda, M.G. and Wright, R.H.G. (2023) CDKN1A/P21 in Breast Cancer: Part of the Problem, or Part of the Solution? *Inter-*

*national Journal of Molecular Sciences*, **24**, Article 17488. https://doi.org/10.3390/ijms242417488

[9] Gui, K., Li, X., Song, J., Li, A., Fan, J. and Huang, L. (2025) Ubiquitin Ligase MDM2 Regulates Chondrocyte Damage, Ferroptosis, and Oxidative Stress by Modulating the Ubiquitination Level of CDKN1A. *International Journal of Rheumatic Diseases*, **28**, e70384. https://doi.org/10.1111/1756-185x.70384

[10] Xu, Q., Chen, Y., Zhang, H., Zhou, K., Zhao, Y., Deng, W., *et al.* (2025) CDKN1A and EGR1 Are Key Genes for Endoplasmic Reticulum Stress-Induced Ferroptosis in Mash. *Free Radical Biology and Medicine*, **236**, 188-203. https://doi.org/10.1016/j.freeradbiomed.2025.05.413

[11] Fisch, K.M., Gamini, R., Alvarez-Garcia, O., Akagi, R., Saito, M., Muramatsu, Y., *et al.* (2018) Identification of Transcription Factors Responsible for Dysregulated Networks in Human Osteoarthritis Cartilage by Global Gene Expression Analysis. *Osteoarthritis and Cartilage*, **26**, 1531-1538. https://doi.org/10.1016/j.joca.2018.07.012

[12] Zhou, N., Peng, L., Luo, Q., Yin, T., Sun, H., Zhang, Y., *et al.* (2025) FerrDb V3: Expanding the Manually Curated Resource for Regulators and Disease Associations from Ferroptosis to Regulated Cell Death. *Nucleic Acids Research*, **54**, D572-D582. https://doi.org/10.1093/nar/gkaf1119

[13] Zhao, Y., Zheng, Y., Li, H., Li, Y., Wang, R., Cai, Y., *et al.* (2025) Protein Folding Dependence on Selenoprotein M Contributes to Steady Cartilage Extracellular Matrix Repressing Ferroptosis via PERK/ATF4/CHAC1 Axis. *Osteoarthritis and Cartilage*, **33**, 261-275. https://doi.org/10.1016/j.joca.2024.10.005

[14] Cao, S., Wei, Y., Xiong, A., Yue, Y., Yang, J., Wang, D., *et al.* (2025) Paeonol Inhibits ACSL4 to Protect Chondrocytes from Ferroptosis and Ameliorates Osteoarthritis Progression. *Journal of Orthopaedic Translation*, **50**, 1-13. https://doi.org/10.1016/j.jot.2024.10.005

[15] Zhao, X., Lin, J., Liu, F., Zhang, Y., Shi, B., Ma, C., *et al.* (2025) Targeting P21-Positive Senescent Chondrocytes via IL-6R/JAK2 Inhibition to Alleviate Osteoarthritis. *Advanced Science*, **12**, e2410795. https://doi.org/10.1002/advs.202410795

[16] Ruan, G., Ying, Y., Lu, S., Zhu, Z., Chen, S., Zeng, M., *et al.* (2023) The Effect of Systemic Iron Status on Osteoarthritis: A Mendelian Randomization Study. *Frontiers in Genetics*, **14**, Article ID: 1122955. https://doi.org/10.3389/fgene.2023.1122955

[17] Yang, T., Yang, X., Wang, G., Jia, D. and Li, Y. (2025) Unraveling the Crucial Role of SDF-1 in Osteoarthritis Progression: IL6/HIF-1α Positive Feedback and Chondrocyte Ferroptosis. *International Immunopharmacology*, **152**, Article 114400. https://doi.org/10.1016/j.intimp.2025.114400

[18] Zhu, Z., Tang, Y., Wu, K., Zhu, F., Luo, Z. and Fu, X. (2025) Expression of Serum Ferroptosis Related Index PTGS2 in Patients with Traumatic Arthritis and Its Correlation with Secondary Cartilage Injury and Diagnostic Efficiency Analysis. *Journal of Orthopaedic Surgery*, **33**.